Princeton Plasma Physics Laboratory

PPPL- 4307

PPPL- 4307

INVESTIGATION OF EBW THERMAL EMISSION AND MODE CONVERSION PHYSICS IN H-MODE PLASMAS ON NSTX

S.J. DIEM, G. TAYLOR, P.C. EFTHIMION, H.W. KUGEL, B.P. LEBLANC, C.K. PHILLIPS, J.B. CAUGHMAN, J.B. WILGEN, R.W. HARVEY, J. PREINHAELTER, J. URBAN, AND S.A. SABBAGH

March 2008

Prepared for the U.S. Department of Energy under Contract DE-AC02-76CH03073.

INVESTIGATION OF EBW THERMAL EMISSION AND MODE CONVERSION PHYSICS IN H-MODE PLASMAS ON NSTX

S.J. DIEM, G. TAYLOR, P.C. EFTHIMION, H.W. KUGEL, B.P. LEBLANC, C.K. PHILLIPS

Princeton Plasma Physics Laboratory, Princeton University
Princeton, NJ 08543, USA

J.B. CAUGHMAN, J.B. WILGEN

Oak Ridge National Laboratory
Oak Ridge, TN 37381, USA

R.W. HARVEY

CompX
Del Mar, CA 92014, USA

J. PREINHAELTER, J. URBAN

Institute of Plasma Physics
Prague, Czech Republic

S.A. SABBAGH

Columbia University
New York, NY 10027, USA

High β plasmas in the National Spherical Torus Experiment (NSTX) operate in the overdense regime, allowing the electron Bernstein wave (EBW) to propagate and be strongly absorbed/emitted at the electron cyclotron resonances. As such, EBWs may provide local electron heating and current drive. For these applications, efficient coupling between the EBWs and electromagnetic waves outside the plasma is needed. Thermal EBW emission (EBE) measurements, via oblique B-X-O double mode conversion, have been used to determine the EBW transmission efficiency for a wide range of plasma conditions on NSTX. Initial EBE measurements in H-mode plasmas exhibited strong emission before the L-H transition, but the emission rapidly decayed after the transition. EBE simulations show that collisional damping of the EBW prior to the mode conversion (MC) layer can significantly reduce the measured EBE for $T_e < 20$ eV, explaining the observations. Lithium evaporation was used to reduce EBE collisional damping near the MC layer. As a result, the measured B-X-O transmission efficiency increased from < 10% (no Li) to 60% (with Li), consistent with EBE simulations.

1. Introduction

Electromagnetic waves in the electron cyclotron (EC) range of frequencies have been used in tokamaks to provide localized EC resonance heating (ECRH) and local EC current drive (ECCD). However, spherical tokamaks (ST) and reverse field pinches (RFP) have low magnetic fields and high electron densities such that the plasma is typically overdense, that is $\omega_{pe} >> \Omega_{ce}$, where ω_{pe} and Ω_{ce} are the electron plasma and cyclotron frequencies, respectively. In overdense devices, the propagation of EC waves beyond the plasma edge is cut off and prohibits the use of ECRH and ECCD. A possible alternative for these overdense devices is the electrostatic electron Bernstein wave (EBW). Unlike EC waves, EBWs do not experience a density cutoff and are readily absorbed/emitted at EC resonances. The EBW cannot propagate in vacuum and must couple to electromagnetic waves (either O- or X-mode).

Currently, the O-mode to slow X-mode to EBW (O-X-B) double mode conversion process is being considered for future low-field-side (LFS) power injection in the ST. For this process, an O-mode is obliquely launched into the plasma and propagates until it is converted to the slow X-mode branch at the plasma cutoff layer where $\omega=\omega_{pe}$. The X-mode then propagates towards the plasma edge until it reaches the upper hybrid resonance (UHR) layer where $\omega=\omega_{UH}=((\omega_{pe})^2+(\Omega_{ce})^2)^{1/2}$. At the UHR layer, the slow X-mode is converted to an EBW. The EBW then propagates towards the plasma center until it is absorbed at an EC resonance. The O-X-B transmission function is given by [1,2]:

$$T_{OXB}\left(n_\perp, n_\parallel\right) = \exp\left\{-\pi k_o L_n \sqrt{\left(Y/2\right)}\left[2\left(1+Y\right)\left(n_{\parallel,opt} - n_\parallel\right)^2 + n_\perp^2\right]\right\} \tag{1}$$

$$L_n = \left|\frac{n_e}{dn_e/dR}\right| \tag{2}$$

$$n_{\parallel,opt}^2 = \frac{Y}{\left(Y+1\right)} \tag{3}$$

where L_n is the density scale length at the mode conversion (MC) layer, $n_\parallel$ and $n_\perp$ are the indices of refraction parallel and perpendicular to the magnetic field, and $Y=\Omega_{ce}/\omega$. At an optimum $n_{\parallel,opt}$ (eqn. (3)), complete conversion of the O-mode to X-mode occurs. The B-X-O transmission efficiency can be improved by reducing L_n to make the angular coupling window larger.

NSTX studies plasma with n_e=10^{19}-10^{20} m^{-3}, but with relatively low magnetic fields, B < 0.6 T, so that the first several EC harmonics are overdense. The current focus of EBW research on NSTX is to access the feasibility of an EBW heating and CD system for future ST devices operating in H-mode, such as a Spherical Tokamak Component Test Facility (ST-CTF). Numerical modeling has shown that by adding 1 MA of off-axis EBWCD to an ST-CTF plasma, the stability is significantly increased by increasing the β_n and β_t stability limits [3].

The EBW emission (EBE) physics of B-X-O MC is essentially the reverse process of the O-X-B MC process used for heating [4], except that the introduction of RF power may excite lossy nonlinear phenomena like parametric decay [5, 6]. The present work focuses on investigating emission via the B-X-O mode conversion process in H-mode plasmas in order to economically assess the feasibility of O-X-B coupling. Section 2 describes the EBE diagnostic on NSTX and the EBE simulation code. Section 3 presents some H-mode experimental results and section 4 discusses the implications for this research.

2. EBE Radiometer and Simulation Code

EBE measurements on NSTX are acquired with two remotely microwave antennas measuring fundamental, second, and third harmonic emission (8-36 GHz). The antennas are mounted outside of the vacuum vessel roughly 50 cm from the plasma edge and connected to dual channel absolutely calibrated heterodyne radiometer systems [7]. Since EBW emission is at blackbody levels in NSTX plasmas, the measured radiation temperature, T_{rad}, is equal to the local T_e at the EBW emission location if the B-X-O transmission efficiency is 100%. The measured emission is simulated with an EBE simulation code developed by Preinhaelter [8]. The code launches 41 rays to simulate the antenna pattern of the EBE diagnostic. A full-wave code is used to calculate the transmission efficiency of the O-X-B mode conversion process and is coupled to a 3D ray-tracing code. The EBE code inputs are the T_e and n_e profiles from Thomson scattering as well as the magnetic equilibria provided by EFIT. Collisions are incorporated into the EBE code with a BGK collision operator.

3. H-mode EBE Results

Initial B-X-O emission measurements in H-mode NSTX plasmas (I_p= 1 MA, $n_e(0)$=3-6x10^{19} m^{-3}, $T_e(0)$ = 0.9 keV, and $B_t(0)$ = 4 kG) exhibited a period of strong emission before the L-H transition, but the emission rapidly decayed after the transition. This trend was observed for all measured EC harmonics, with the details for 24 GHz emission shown in figure 1. The large fluctuation levels, > 50%, shown in figure 1 correlate to fluctuations in L_n at the MC layer, resulting in B-X-O transmission efficiency fluctuations > 20%.

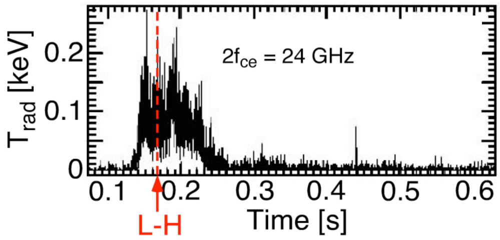

Figure 1. The time evolution of T_{rad} for 24 GHz emission is shown as a function of time. The L-H transition is indicated by the vertical dashed line.

For times less than 0.25 s, the B-X-O MC layer ($\omega = \omega_{UH}$) is located at the last closed flux surface (LCFS) where T_e > 20 eV. Shortly after the L-H transition (t > 0.25 s), the B-X-O MC layer shifted outside of the LCFS where T_e < 10 eV (figure 2). The B-X-O transmission efficiency in these H-mode plasmas peaks at 20% and then falls to << 10% during the current flattop.

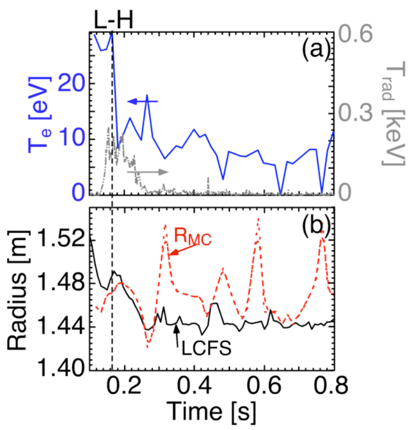

Figure 2. (a) T_e (solid line) at the 24 GHz MC layer is plotted versus time for an NSTX H-mode discharge. (b) The position of the LCFS is compared with the radial location of the MC layer (R_{MC}).

If T_e< 20 eV at the MC layer, EBW collisional damping effects can become significant. The EBE simulation code was used to model second harmonic emission at 24 GHz. Simulations without collisional effects predict a measured T_{rad} of 0.8 keV throughout the H-mode phase of the discharge, significantly disagreeing with the behavior of the measured T_{rad} (figure 1). By including collisional damping of the EBW prior to mode conversion, the EBE simulation results follow the rapid decay trend shown in figure 1. Details in the EBE simulations show that the ray intensity is decreased from 60% to 20% due to collisional damping for t > 0.25 s.

Lithium evaporation [9] was used to reduce EBW collisional damping in the plasma scrape off and in the vicinity of the LCFS. The evaporation rate was increased from 0 to 19 mg/min to reduce n_e, moving the MC layer to the LCFS where T_e is higher. The central T_e remained relatively constant during the experiment as the Li evaporation was increased. With Li edge conditioning, an increase in T_e near the fundamental MC layer from 10 eV (no Li) to 20 eV (with Li) was observed. A significant increase in the measured T_{rad} from < 50 eV to > 450 eV for f_{ce}=18 GHz (near axis emission) was observed during the Li evaporation scan. In addition, emission from all harmonics remained at a constant level throughout the discharge. The inferred B-X-O transmission efficiency increased from < 10% (no Li) to 60% (with Li). Results from the EBE simulations show that the ray intensity increased from 40% to 80% with edge conditioning. Good agreement between the measured and simulated T_{rad} indicate that significant reduction of EBW collisional damping occurs with edge conditioning. Similarly, the B-X-O transmission for second harmonic emission increased from < 10% to 50% with Li edge conditioning.

An experimental scan of the B-X-O transmission efficiency window was performed while edge conditioning with Li. The target H-mode plasma was repeated and the antennas were moved to a new position between discharges. The measured and simulated toroidal and poloidal angle of maximum transmission agreed within several degrees for both fundamental and second harmonic emission (figure 3 (a) and (b)).

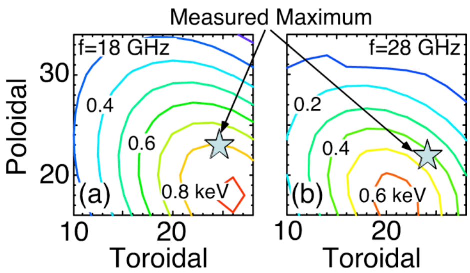

Figure 3. The simulated T_{rad} as a function of toroidal and poloidal angle is plotted for (a) fundamental emission at 18 GHz and (b) second harmonic emission at 28 GHz. The location of the measured angle of maximum emission is indicated by a star.

The simulated maximum T_{rad} was higher than the measured T_{rad} with values of 0.9 keV and 0.6 keV for fundamental and second harmonic emission, respectively, compared to measured values of ~0.6 keV and ~0.4 keV, respectively.

4. Discussion

This work has significant implications for future ST devices that may use EBWCD, such as an ST-CTF, when the O-X-B MC layer is shifted outside the plasma to a region where $T_e < 20$ eV. For these conditions, O-X-B heating and CD may become inefficient due to significant EBW collisional losses. This work has demonstrated that using edge conditioning to increase T_e outside the LCFS can significantly reduce these losses. In heating experiments, enough power will be flowing through the MC layer that T_e may increase enough to mitigate any possible EBW collisional damping. In addition, fluctuations in L_n can lead to > 20% fluctuations in B-X-O transmission efficiency which is not desirable for RF coupling. Moving the MC layer even further inside the LCFS, where density fluctuations are lower, may significantly reduce these fluctuations and improve RF coupling.

Acknowledgments

Research supported by USDOE DE-AC02-76CH03073, DE-FG02-91ER-54109, DE-FG03-02ER-54684, DE-FG02-99ER-54521 and a grant to encourage innovations in fusion diagnostic systems.

References

1. E. Mjolhus, *J. Plasma Phys*. **31**, 7 (1984)
2. F.R. Hansen, J.P. Lynoc, C. Maroli, and V. Petrillo, *J. Plasma Phys*. **39**, 319 (1988)
3. Y-K. M. Peng, et al., *PPCF*, **47** (2005)
4. A.K. Ram, A. Bers, and C.N. Lashmore-Davies, *Phys. Plasmas* **9**, 409 (2002)
5. Ya. N. Istomin and T.B. Leyser, *Phys. Plasmas* **2**, 2084 (1995)
6. V.K. Yadav and D. Bora, *Phys. Plasmas* **11**, 3409 (2004)
7. S.J. Diem, et al., Rev. Sci. Instrum. 77 (2006)
8. J. Preinhaelter, et al., *Rev. Sci. Instrum.* **77**, 10F524 (2006)
9. H.W. Kugel, et al., *J. of Nucl. Mater*. **363-365**, 791 (2007)

The Princeton Plasma Physics Laboratory is operated
by Princeton University under contract
with the U.S. Department of Energy.

Information Services
Princeton Plasma Physics Laboratory
P.O. Box 451
Princeton, NJ 08543

Phone: 609-243-2750
Fax: 609-243-2751
e-mail: pppl_info@pppl.gov
Internet Address: http://www.pppl.gov